LARGE EDDY SIMULATION OF THE EFFECT OF HEAT FLUX ON POLLUTANT DISPERSION IN AN URBAN STREET CANYON

(Date received: 14.4.09)

Andy Chan[1], Eric Cheung[2] and Pradeep Siddheshwar[3]
[1] Department of Chemical and Environmental Engineering,
University of Nottingham (Malaysia Campus),
Jalan Broga, 43500 Semenyih, Selangor Darul Ehsan
[2]Department of Mechanical Engineering,
The University of Hong Kong, Pokfulam, Hong Kong
[3]Department of Mathematics, Bangalore University,
Central College Campus, Bangalore 560001, Karnataka, India
E-mail: [1]andy.chan@nottingham.edu.my

ABSTRACT

The effect of heat flux on pollutant dispersion in an urban street canyon with fixed aspect ratio of 1 is investigated under four different heating configurations: windward heating, leeward heating, ground heating, and walls and ground heating, using large-eddy simulations (LES). For each heating configuration, the Reynolds number is varied from 400 to 3,000 and the Grashof number from 80,000 to 800,000. The retention value (the ratio of pollutant remaining inside canyon to the total pollutant emitted) is used to compare the effect of heating on pollutant dispersion under each heating configuration. Numerical results show that the wind flow patterns, pollutant dispersion patterns and retention values depend not only on the canyon aspect ratio and inflow wind speed, but also on the strength of heating and the heating configuration. The most significant effect arises from the case of windward heating when the main vortex rotating in the clockwise direction is countered by the buoyancy effect near the windward wall; the pollutant accumulated near the leeward wall is therefore decreased. On the other hand, no significant change is observed in the wind flow and pollutant dispersion pattern for the cases of leeward, ground and walls and ground heating. As the strength of heating is increased gradually, the strength of the vortex rotating in the counter-clockwise direction at the lower corner of the windward wall also increases; this causes the pollutant to accumulate near the windward wall. A further increase in the strength of heating causes the formation of a third vortex above the second one, the pollutant accumulated near the windward wall is therefore increased.

Keywords: *Canyon Aspect Ratio; Grashof Number; Heat Flux; Large-eddy Simulation; Pollutant Dispersion; Urban Street Canyon*

1.0 INTRODUCTION

Urban heat island heat is a serious problem in many modern cities. The situation is worsened by the continuous increase in traffic and the pollutants it accompanies. That means pedestrians in the streets breathe in polluted air in a very hot environment. It is of major importance to find out how the pollutants are dispersed in the urban streets.

There are basically two approaches in studying the urban canyon flow problem: field measurements or wind tunnel experiments [1-3], and computational modelling [4, 5]. Field measurements and experimentations provide useful information on airflow characteristics and pollutant distribution in real situations. However, there are so many parameters involved and thus it is impossible to control. These parameters include building geometry, street dimension, traffic flow rate, thermal effect *etc*. Wind tunnel experiments offer the advantages of being able to control the parameters individually and the results are often used to verify the validity of computation models. The problem of wind tunnel experiments and field surveys is that they are expensive to conduct. As for the second option, it has been shown by many researchers that computational simulations agree reasonably well with field measurements and wind tunnel experiments using minimum cost [1, 3, 6].

According to Oke [7], the characteristic wind flow pattern in an urban street canyon can be classified into three regimes: namely isolated roughness flow, wake interference flow, and skimming flow. Many researchers have studied the three flow regimes using numerical simulations [8]. Subsequent researches have shown that the flow regimes can also be affected by inflow wind speed and canyon geometry which in turns affect the pollutant dispersion patterns [5, 6]. Apart from canyon geometry, the effect of heat flux may also play an important

role in pollutant dispersion in urban street canyons. One of these parameters is the addition of heat: It has also been shown by wind tunnel experiments and numerical simulations that the airflow in and above the canyon can be affected by thermal stratification [9-12]. Heat flux comes into play through solar irradiation, human or industrial activities or urban heat, which intuitively might affect the local atmospheric stability and the convective flow patterns within the city. Moreover heat exchanges in cities are the main cause of urban heat island effects. Urban heat island has serious implications in modern cities development and it has been significantly neglected in previous works. It is therefore important to understand how heat flux affects the wind flow and pollutant dispersions within a city.

Large eddy simulation (LES) is used in the present study to simulate the flow field and the pollutant dispersion pattern. LES technique is selected in the study because the firstly it does not involve any modelling in the large scale and thus is considered exact and secondly, conventional *k*-ε or *k*-ω model is known to over-predict turbulent kinetic energy in shear zones and near boundaries, which is important in our case. It has been shown in previous studies that LES is very useful in the study of urban canyon flows [5].

In our study, all large-scale quantities are computed while all the small-scale quantities are modelled using Smagorinsky subgrid scale model. Four different heating configurations are simulated to compare the effect in various situations, namely: windward heating, leeward heating, ground heating, and walls and ground heating. For each heating configuration, the Reynolds number are varied from 400 to 3000 to study the effect of heating under various inflow speed, Grashof number are varied from 0 to 800000 to study the effect of heating under various heating strength.

2.0 GOVERNING EQUATIONS

2.1 Governing Equations for the Wind Flow

For an incompressible Newtonian fluid with Boussinesq's approximation for buoyancy force, the governing equations for two-dimensional LES in dimensionless forms are

$$\frac{\partial \overline{u_i}}{\partial \overline{x_i}} = 0 \tag{1}$$

$$\frac{\partial \overline{u_i}}{\partial t} + u_j \frac{\partial \overline{u_i}}{\partial x_j} = -\frac{\partial \overline{p}}{\partial x_i} + \left(\frac{1}{Re} + \frac{1}{Re_t}\right)\frac{\partial^2 \overline{u_i}}{\partial x^2_j} + \left(\frac{\partial}{\partial x_j}\frac{1}{Re_t}\right)\left(\frac{\partial \overline{u_i}}{\partial x_j} + \frac{\partial \overline{u_j}}{\partial x_i}\right) + \frac{Gr}{Re^2}\delta_{i2} \tag{2}$$

$$\frac{\partial \overline{T}}{\partial t} + \overline{u_j}\frac{\partial \overline{T}}{\partial x_j} = \left(\frac{1}{Pr}\frac{1}{Re} + \frac{1}{Pr_t}\frac{1}{Re_t}\right)\frac{\partial^2 \overline{T}}{\partial x_j \partial x_j} + \frac{\partial}{\partial x_j}\left(\frac{1}{Pr_t}\frac{1}{Re_t}\right)\frac{\partial \overline{T}}{\partial x_j}, \tag{3}$$

where over-bars represent filtered variables. The dependent variables u_i, p, and T represent velocity components, pressure and temperature respectively. The independent variables x_i and t represent space components and time. The parameters Re = UL/ν, Gr = $g\beta\Delta TL^3/\nu^2$, and Pr = ν/α denote the global Reynolds number, Grashof number and Prandtl number respectively. $Re_t = UL/\nu_t$ and $Pr_t = \nu_t/\alpha_t$ denote the subgrid scale turbulent Reynolds number and turbulent Prandtl number respectively with ρ, ν, g, β, and α being density, kinematics viscosity, gravitational acceleration, thermal expansion coefficient, and thermal diffusivity respectively, while ν_t and α_t denote the sub-grid scale eddy viscosity and eddy thermal diffusivity. The Einstein's summation convention is adopted and 2 is the vertical direction.

The closure for Equations (1) to (3) is then expressed non-dimensionally as

$$\frac{1}{\mathrm{Re}_t} = \frac{1}{2} C_s^2 \Delta^2 \left| \frac{\partial \overline{u_i}}{\partial x_j} + \frac{\partial \overline{u_j}}{\partial x_i} \right|, \tag{4}$$

with C_s being the Smagorinsky constant for LES. The filtered length-scale Δ, is determined from the root for the filters in both directions.

2.2 Pollutant Dispersion Equation

The filtered normalised transport equation of a passive scalar based on Fick's law of diffusion is

$$\frac{\partial \overline{C}}{\partial t} + \mathrm{uj}\frac{\partial \overline{C}}{\partial x_j} = \left(\frac{1}{Sc}\frac{1}{Re} + \frac{1}{Sc_t}\frac{1}{Re_t}\right)\frac{\partial^2 \overline{C}}{\partial x_j^2} + \frac{\partial}{\partial x_j}\left(\frac{1}{Sc_t}\frac{1}{Re_t}\right)\frac{\partial \overline{C}}{\partial x_j}, \tag{5}$$

with C representing the pollutant concentration, where Sc is the Schmidt number and Sc_t is the sub-grid scale Schmidt number.

The retention value R is used to study the efficiency of pollutant dilution in the canyon. It is defined as the ratio of pollutant trapped inside the canyon to that being released during the same period of time. The retention value is calculated by

$$R = \frac{\text{concentration of pollutant found in canyon}}{\text{total emission of pollutant from source}} \tag{6}$$

2.3 Boundary Conditions

A logarithmic wind profile is introduced at the inlet surface without any turbulence excitation and the outlet is of outflow condition. All building surfaces and datum surfaces are set as no-slip boundaries while free-slip boundary is used for top of the computational domain. The boundary conditions for velocity and temperature are listed in Table 1 and 2 respectively as in Figure 1, where u^* is the frictional velocity, κ is the Von Karman's constant and z_0 is the roughness length of the ground.

Table 1: Velocity boundary conditions used for the computation

Surface	Nature	Input value
A to J	Ground	No-slip boundary condition ($u_i = 0$)
JK	Outlet	Outflow ($\frac{\partial u}{\partial x} = 0$)
KL	System wall	Free-slip boundary condition ($p = 0$)
LA	Inlet	Logarithmic wind profile ($u = \frac{u^*}{\kappa} \log \frac{z}{z_0}$)

Table 2: Temperature boundary condition used for the computation

Surface	Nature	Input value
A to J (except DE, EF FG)	Building wall or ground	Insulated (T_0)
DE	Windward wall	Wall temperature, insulated otherwise
EF	Canyon ground	Ground temperature, insulated otherwise
FG	Leeward wall	Wall temperature, insulated otherwise
JK	Outlet	Free
KL	System wall	Atmospheric (T_a)
LA	Inlet	Free

2.4 Numerical Scheme

The filtered dimensionless Equations 1 to 3 are solved numerically using finite difference method with third-order upwind scheme on structured grids. The staggered marker-and-cell method for mesh development and Poisson pressure equations are adopted for pressure component using composite domain technique. The retention value is calculated using numerical integration. The solution convergence criterion depends on the Courant-Friedrichs-Lewy (CFL) number

$$N_{CFL} = \text{Max}\left(\frac{\Delta t|u|}{\Delta x}, \frac{\Delta t|v|}{\Delta y}\right) < 1. \quad (7)$$

The code had been validated with the standard drive-lid cavity test with a number of meshes and excellent agreements have been obtained with experimental and numerical data as presented in Lai and Chan [13]. Subsequently the work has also been compared with Xie *et al*. [11] and Yee *et al*. [14] and again good agreements have been achieved.

2.5 Model Configurations

A 2D computation domain with dimensionless length of 15 dimensionless units and height of 5 units is used to simulate all the cases as in Figure 1. B1 and B2 represent upwind and downwind building respectively. The area bounded between B1 and B2 (DEFG) represents the urban street canyon. The entry length (AB) is 4 units while the length from the downwind building to outlet (IJ) is 10 units. For the present cases, the height and width of the two buildings are fixed at 1 unit and the width of the canyon is 1 unit, giving a canyon aspect ratio of 1. The total number of cells involved is approximately 500000, varying from case to case.

A grid-dependency study has been performed prior to the simulations and it is found that with a grid size of 500000, the simulations are grid-independent. Moreover the grid-size is calculated based on Pope [15] based on the $\Delta x/\Delta = 1/2$ for a box filter.

We focus mainly on building blocks with a canyon ratio of 1 only with the following reasons. Firstly it has been shown in previous works [5, 11] that the square canyon is the threshold between skimming flow and wake-interference flow regimes [7]. This represents a critical building geometry system where pollutant dispersion is most difficult. Secondly we intend to focus on the effect of heat flux on the air flow and pollution dispersion pattern. Thirdly the square canyon represents the benchmark for most canyon flow studies.

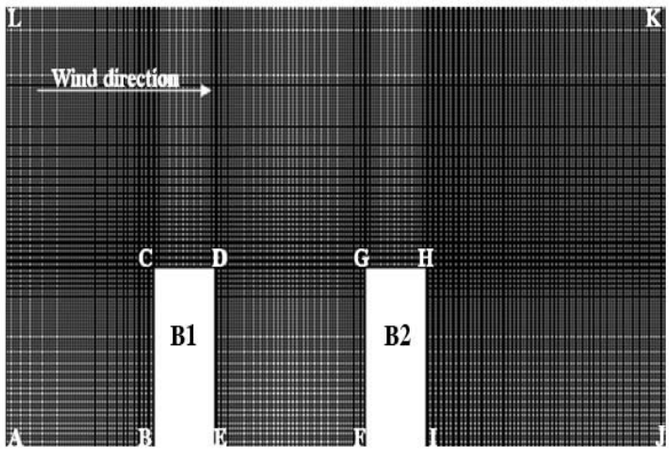

Figure 1: Schematic diagram of the meshed computation domain

3.0 RESULTS AND DISCUSSIONS

Four heating configurations are simulated including windward, leeward, ground and walls and ground heating. Each of this is to simulate the effect solar radiation direction on the microclimate inside the street canyon. For each heating configuration, Re = 400 and Gr = 0 (no heating) is first obtained, then the Grashof number is increased in a step size of 80000 from 0 to 800000. On the other hand, the work is to demonstrate the physical effect of forced convection on the pollutant dispersion. The Reynolds number is increased in a step size of 400 (200 for the last step) to obtain the cases of all the heating configurations at Re = 800 (laminar), Re = 2000 (transition), and Re = 3000 (fully turbulent).

3.1 Wind flow pattern

3.1.1 Windward heating

Various temperature differences based on the Grashof number are applied between the windward wall (wall of building B2 facing the canyon) and the surrounding air. The wind flow pattern inside the canyon is observed to be strongly affected by the heat flux in the case of windward heating. The streamline plots for the cases of Re = 400 with Gr varies from 0 to 800000 are shown in Figure 2. For the case of no heating, the canyon is dominated by a clockwise rotating vortex accompanied by small secondary counter rotating vortices at each corner (Figure 2a). As the strength of heating increases, the vortex at the windward corner becomes bigger and eventually merges with the vortex at the leeward corner (Figure 2b). The strength of the merged vortex is increased by a further increase in heating; and finally, as the merged vortex becomes dominant inside the canyon, a new vortex rotating clockwisely is formed near the top of the leeward wall at the same time (Figure 2c).

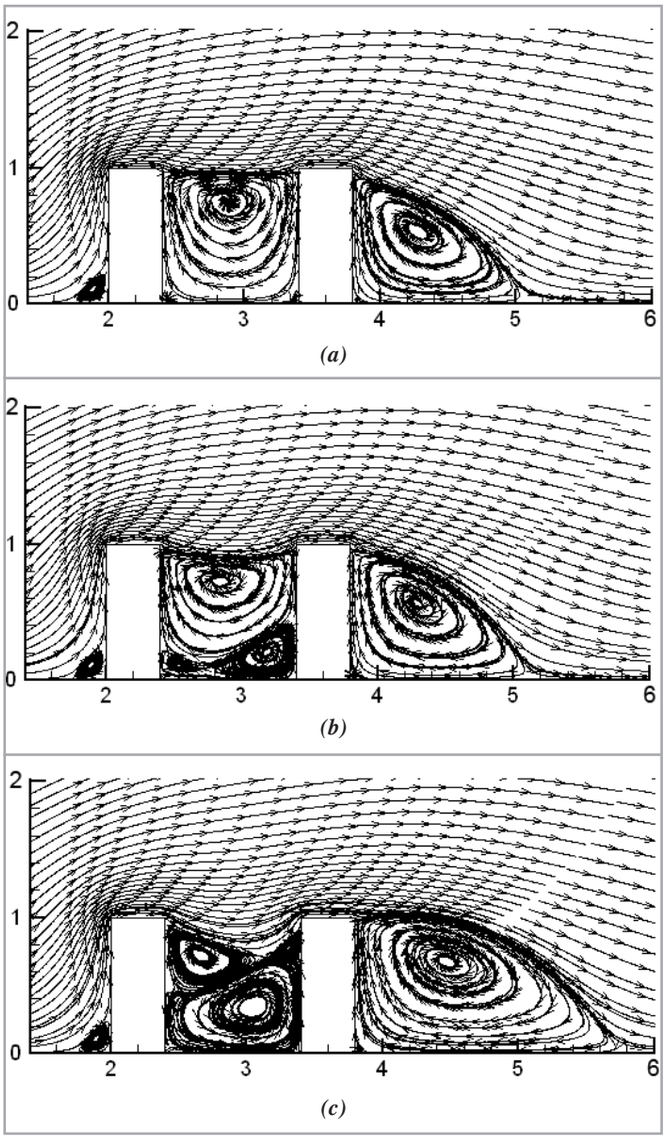

Figure 2: Variation of the streamline at Re = 400 with windward wall heated. Gr = 0, 400,000, 800,000 from Figures (a) to (c)

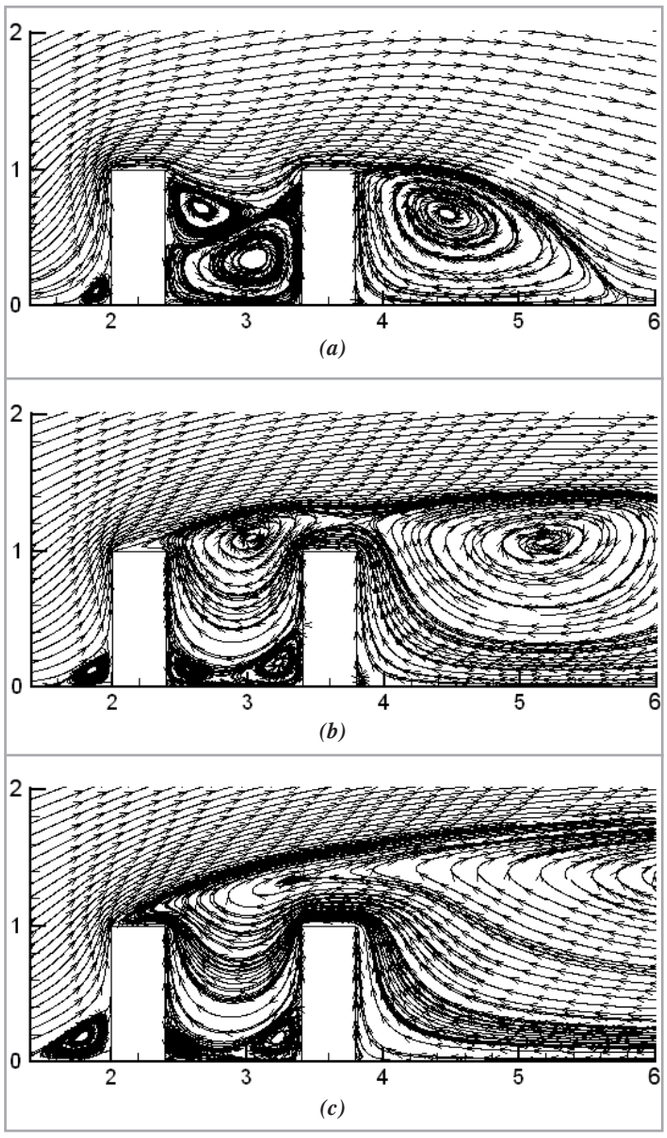

Figure 3: Variation of streamline at Gr = 800,000 with windward wall. Re = 400, 2,000, 3,000 from Figures (a) to (c)

The effect of heat flux on wind flow pattern can be explained by the buoyancy force acting on the air near the windward wall. As long as the temperature on the windward wall is higher than the surrounding air, there is a buoyancy force acting on the air near the windward wall which tends to weaken the clockwise rotating vortex originally dominating in the canyon, while it tends to increase the velocity of the vortex formed at the lower corner of windward wall at the same time. For a fixed Reynolds number, the relative magnitude of the buoyancy force depends on the Grashof number only. The Grashof number increases with the temperature difference between the heated windward wall and the surrounding air. The buoyancy term eventually becomes the dominant term and so the counterclockwise rotating vortex dominates the canyon.

As the Reynolds number increases from 400, the effect of heat flux on the wind flow pattern becomes less significant even at large Grashof number (Figure 3a). The canyon is dominated by the clockwise rotating vortex originally formed without heating, and this vortex starts move up at Re = 2000 (Figure 3b). A further increase of Reynolds number causes the clockwise rotating vortex to merge with the downwind vortex (Figure 3c).

The relative magnitude of the buoyancy term decreases as the square of Reynolds number, while that of the inertia term remains unchanged. Therefore, the effect of heat flux on wind flow at high Reynolds number is less significant than at low Reynolds number. Eventually as the Reynolds number becomes large enough, the inertia term becomes the dominant term in Equation 2, so the canyon is dominated by the clockwise rotating vortex.

3.1.2 Leeward heating

Similar to the previous case, various temperature differences are applied between the leeward wall (wall of building B1 facing the canyon) and the surrounding air. There is no observable change of wind flow pattern inside the canyon when different temperature difference is applied to the leeward wall (Figures 4a and b). The buoyancy force acting on the air near the leeward wall tends to strengthen the clockwise rotating vortex along the leeward wall and therefore only the strength of vortex increases with temperature difference between the wall and surrounding air.

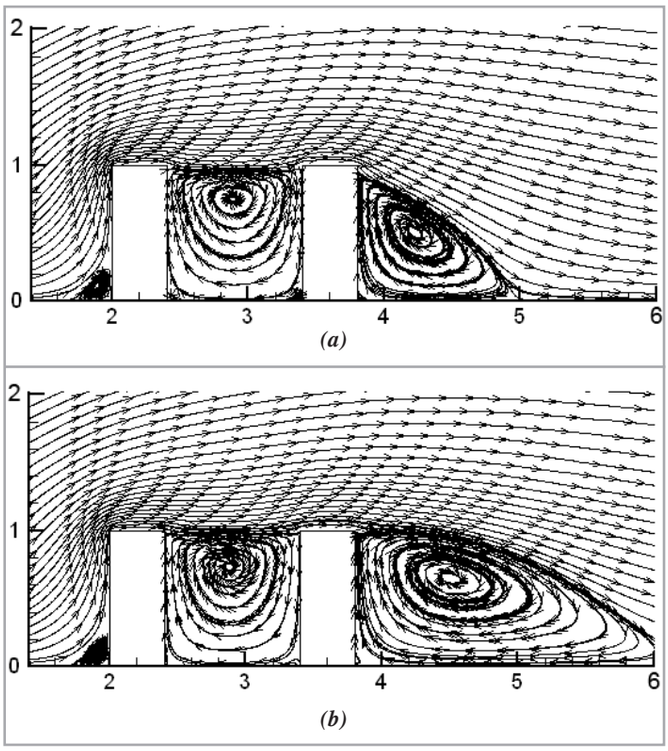

Figure 4: Variation of streamline at Re = 400 with leeward wall heated. Gr = 0, and 800,000 from Figures (a) to (b)

3.1.3 Ground heating

Similar to the cases of leeward heating, there is no significant change observed in the wind flow pattern caused by temperature difference variation (Figure 5). The buoyancy force acts on the air near the surface on the canyon ground evenly and there is no tendency of strengthening or weakening the main vortex.

For larger Reynolds numbers even at the largest Grashof number simulated, the effect of heat flux becomes less significant (Figure 5). This is because the relative magnitude of the buoyancy term becomes insignificant at large Reynolds numbers, the flow in the canyon is therefore dominated by the main vortex.

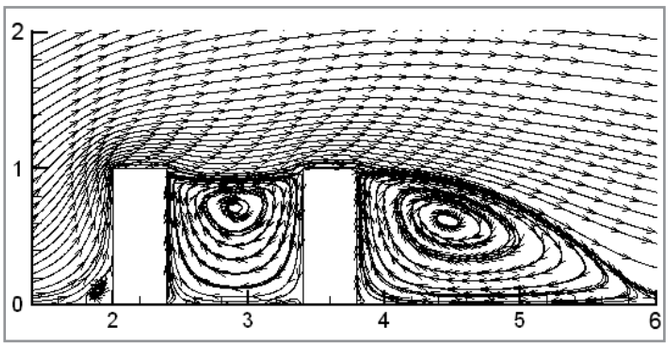

Figure 5: Variation of streamline at Re = 400 with canyon ground heated. Gr = 800,000

3.1.4 Walls and ground heating

This can be regarded as the combination of the three previous cases. The two walls facing the canyon and the canyon ground are maintained at the same temperature, which is higher than the surrounding air. Similar to the cases of leeward heating and ground heating, there is no significant change observed in the wind flow pattern caused by temperature difference variation (Figure 6). The buoyancy force generated by the heat flux on leeward wall tends to strengthen the main vortex, while that on the windward tends to weaken it, the resultant wind flow pattern in canyon is therefore similar to the cases of ground heating.

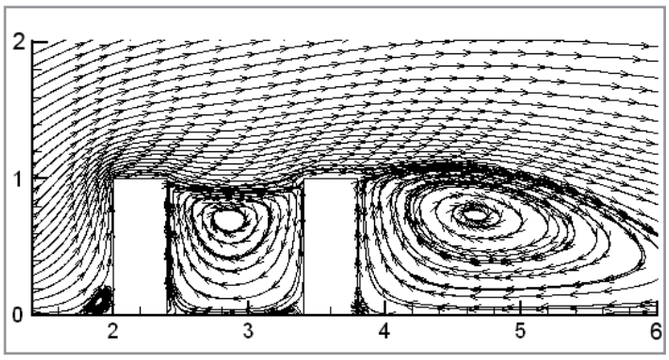

Figure 6: Variation of streamline at Re = 400 with walls and ground heated. Gr = 800,000

For larger Reynolds number even at the largest Grashof number, the effect of heat flux becomes less significant (Figure 7). This is because the relative magnitude of the buoyancy term becomes insignificant and eventually negligible at large Reynolds number, the flow in the canyon is therefore dominated by the main vortex again.

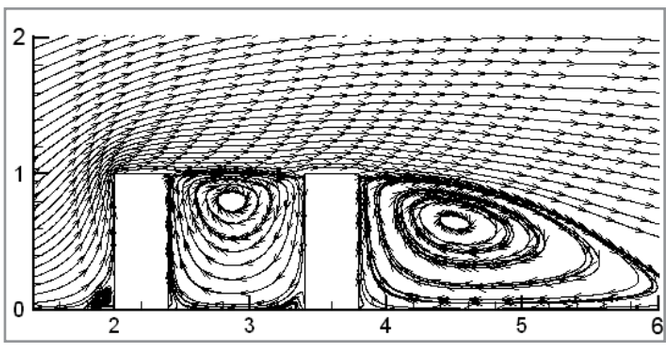

Figure 7: Variation of streamline at Gr = 800,000 with walls and ground heated. Re = 3,000

3.2 Pollutant dispersion pattern

Pollutant dispersion pattern is mainly affected by the wind flow pattern which changes significantly in the case of windward heating but remains unchanged in the other three heating configurations. The pollutant concentration is considered as a passive scalar and is dimensionless. The initial concentration is unity. It is important to note that despite similarity in flow pattern, the flow velocities are different and this is anticipated to lead to different pollutant concentration profile. When there is no heating at all, pollutant is concentrated near the leeward wall (Figure 8a) due to the circulation inside the vortex. When a temperature difference is applied between the windward wall and surrounding air, the concentration of the pollutant near the leeward wall decreases. The higher the temperature difference, the lower the pollutant concentration near the leeward wall. Eventually, at sufficient large temperature difference, the pollutant becomes concentrated near the windward wall (Figure 8b).

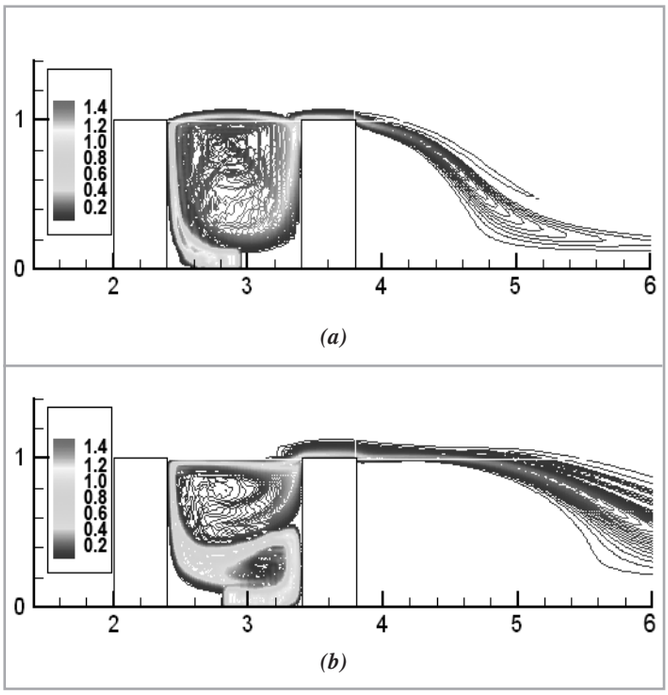

Figure 8: Pollutant dispersion pattern when the windward wall is heated. Re = 3000, Gr = (a) 0, (b) 800,000

For the case of leeward heating, the clockwise rotating vortex is strengthened by the buoyancy force near the leeward wall, there is strong mixing of pollutant inside the canyon, and the pollutant is concentrated near both walls (Figures 9a and b). For the cases of ground heating and walls and ground heating, due to symmetrical heating, there is no observable change in the wind flow pattern and therefore the pollutant dispersion pattern (Figures 9c and d).

The effect of heating on the pollutant dispersion pattern is similar at difference Reynolds number, only the significance decreases with increasing Reynolds number. This can be deduced from the buoyancy term in Equation 3, whose coefficient increases linearly with Grashof number but decreases with the square of Reynolds number. Therefore, the heating effect becomes insignificant at sufficiently large Reynolds number.

To compare the effect of heating on pollutant dispersion under various heating configurations, the retention value defined in Equation (6) is used. Therefore, the higher the retention value, the more is the pollutant remained in the canyon. The retention value obtained at the same time and Reynolds number for different heating configurations are plotted in Figure 11 to compare the effect of heating on pollutant dispersion under different heating configurations and strength.

At low Reynolds number (Re = 400), the retention value for windward heating increases with increasing Grashof number and it reaches a maximum of value of 1 at Gr = 320000. This means almost all the pollutant emitted remains inside the canyon. The retention value for the cases of leeward heating and ground heating remains more or less unchanged with increasing Grashof number. For the case of all walls and ground heating, the retention value decreases with increasing Grashof number. All these can be explained with the wind patterns found inside the canyon as in the previous subsection.

At higher Reynolds number (Re = 3000), the retention value becomes less and less dependent on heating. This is because as the Reynolds becomes large enough, the coefficient of buoyancy term becomes negligible when compared with other terms, so the wind flow pattern and therefore the pollutant dispersion pattern remains more or less similar to that without heating.

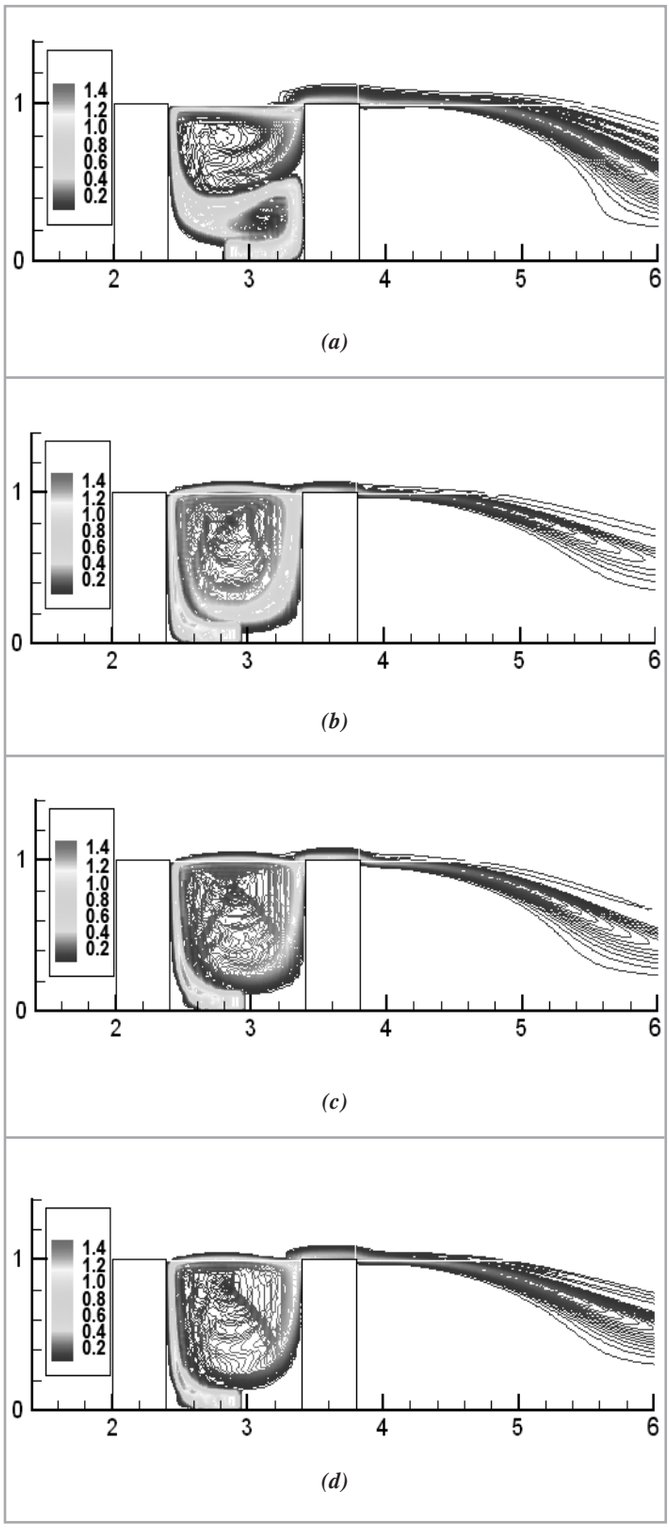

Figure 9: Pollutant dispersion pattern at Re = 3000, Gr = 800,000. (a) Windward heating. (b) Leeward heating. (c) Ground heating. (d) Walls and ground heating

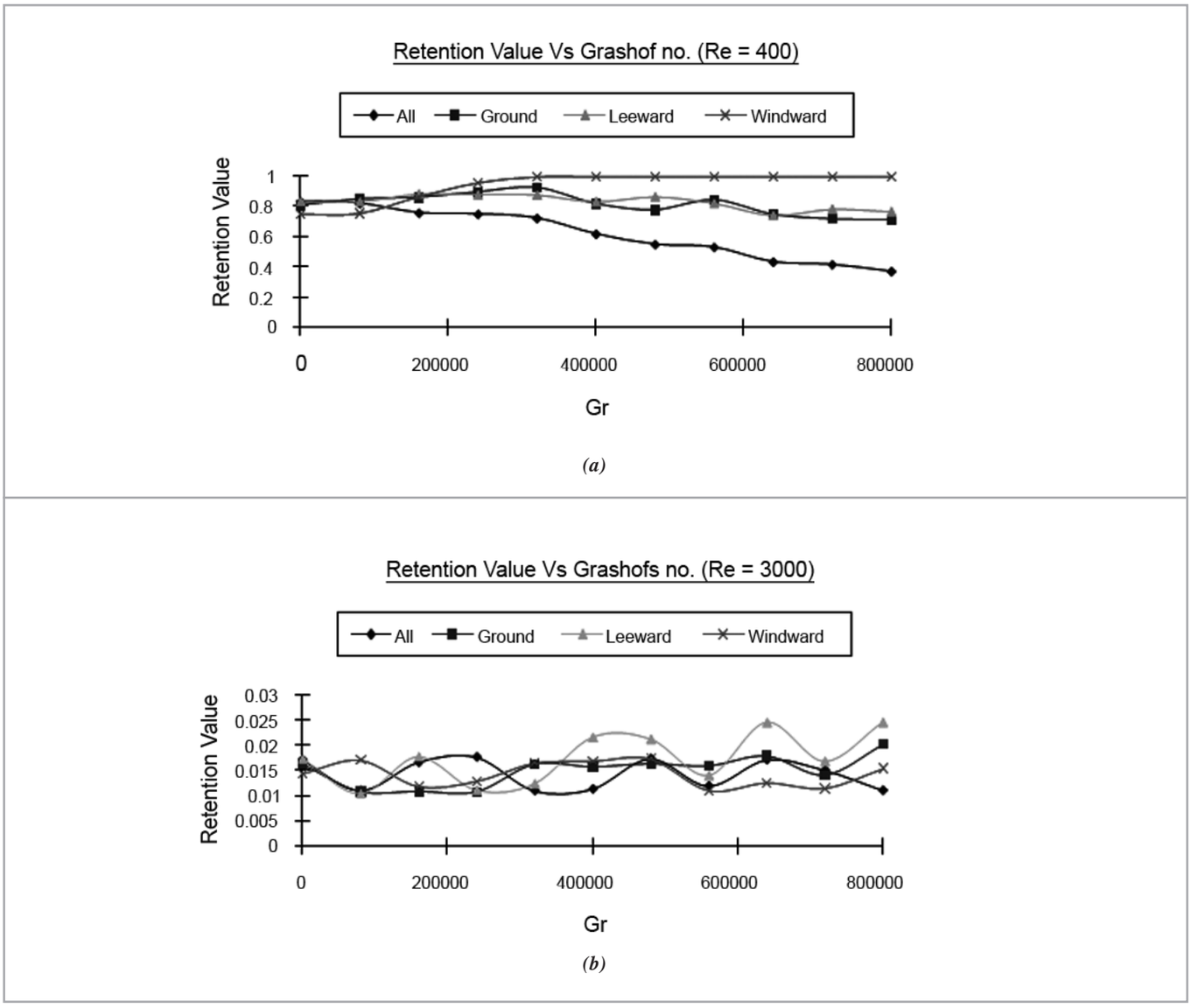

Figure 10: Variations of retention value with Grashofs number under different heating configuration. (a) Re = 400. (b) Re = 3,000

4.0 CONCLUSIONS

The effect of heat flux on wind flow and pollutant dispersion in an urban street canyon is analysed using LES. The wind flow pattern and temperature distribution are solved using LES with the static Smagorinsky's subgrid scale model. The resultant wind field is then used to solve the filtered transported equation of a passive scalar to obtain the pollutant dispersion pattern. Four heating configurations including windward, leeward, ground and walls ground heating are simulated to compare the effect of heating in various situations.

The effect of heating is found to be most significant in the case of windward heating. The buoyancy force acting on the air near the windward tends to weaken the clockwise rotating vortex originally formed inside the canyon; the small counterclockwise rotating vortex at the lower corner of the windward wall is strengthened at the same time. The pollutant is concentrated near the leeward wall in the case of no heating. The concentration decreases as the temperature difference between the windward wall and surrounding air increases, and eventually the pollutant becomes concentrated near the windward wall.

There is no significant change observed in both the wind flow and pollutant dispersion pattern in the cases of leeward, ground and walls and ground heating. In the case of leeward heating, only the strength of the clockwise rotating vortex increase with heating but the shape remains unchanged, this is due to the strengthening effect by the buoyancy force acting on the air near the leeward wall. In the case of ground and walls and ground heating, due to symmetrical heating configuration, both the strength and shape of the vortex remain unchanged. The pollutant dispersion pattern depends on wind flow, and thus there is also no significant change.

A comparison in the retention value shows that windward heating prevents the pollutant dispersion from the canyon, while the other three heating configurations has no significant effect on the pollutant dispersion from the canyon. However, as the buoyancy effect decreases with increasing Reynolds number, the effect of heating becomes insignificant at large Reynolds number no matter which wall is heated. ■

REFERENCES

[1] Tsai M. Y., and Chen K. S. (2004). "Measurements and three-dimensional modeling of air pollutant dispersion in an urban street canyon." Atmospheric Environment, Elsevier, Amsterdam. ISSN 1352-2310. 38(35): pp. 5911-5924.

[2] Kastner-Klein P., Fedorovich E., and Rotach M. W. (2001). "A wind tunnel study of organized and turbulent air motions in urban street canyons." Journal of Wind Engineering and Industrial Aerodynamics, Elsevier, Amsterdam. ISSN 0167-6105. 89(9): pp. 849-861.

[3] Chang C. H., and Meroney R. N. (2001). "Numerical and physical modeling of bluff body flow and dispersion in urban street canyons." Journal of Wind Engineering and Industrial Aerodynamics, Elsevier, Amsterdam. ISSN 0167-6105. 89(14-15): pp. 1325-1334.

[4] Baker J., Walker H. L., and Cai X. (2004). "A study of the dispersion and transport of reactive pollutants in and above street canyons – a large eddy simulation." Atmospheric Environment, Elsevier, Amsterdam. ISSN 1352-2310. 38(39): pp. 6883-6892.

[5] So E. S. P., Chan A., and Wong A. Y. T. (2005). "Large-eddy simulations of wind flow and pollutant dispersion in a street canyon." Atmospheric Environment, Elsevier, Amsterdam. ISSN 1352-2310. 39(20): pp. 3573-3582.

[6] Walton A., Cheng A. Y. S., and Yeung W. C. (2002). "Large-eddy simulation of pollutant dispersion in an urban street canyon – Part I: comparison with field data." Atmospheric Environment, Elsevier, Amsterdam. ISSN 1352-2310. 36(22): pp. 3601-3613.

[7] Oke T. R. (1988). "Street design and urban canopy layer climate." Energy and Building, Elsevier, Amsterdam. ISSN 0378-7788. 11(1-3): pp. 103-113.

[8] Sini J. F., Anquetin S., and Mestayer P. G. (1995). "Pollutant dispersion and thermal effects on urban street canyons". Atmospheric Environment, Elsevier, Amsterdam. ISSN 1352-2310. 30(15): pp. 2659-2677.

[9] Ca V. T., Asaeda T., Ito M., and Armfield S. (1995). "Characteristics of wind field in a street canyon." Journal of Wind Engineering and Industrial Aerodynamics, Elsevier, Amsterdam. ISSN 0167-6105. 57(1): pp. 63-80.

[10] Kim J. J., and Baik J. J. (2001). "Urban street-canyon flows with bottom heating." Atmospheric Environment, Elsevier, Amsterdam. ISSN 1352-2310. 35(20): pp. 3395-3404.

[11] Xie X., Zhen H., Wang J., and Xie Z. (2005). "The impact of solar radiation and street layout on pollutant dispersion in street canyon." Building and Environment, Elsevier, Amsterdam. ISSN 0360-1323. 40(2): pp. 201-212.

[12] Tsai M. Y., Chen K. S., and Wu C. H. (2005). "Three-dimensional modeling of air flow and pollutant dispersion in an urban street canyon with thermal effects." Journal of the Air and Waste Management Association, Air and Waste Management Association, Pittsburgh. ISSN 1047-3289. 55(8): pp. 1178-1189.

[13] Lai M. K. K. and Chan A. (2007), "Large-eddy simulations on indoor/outdoor air quality relationship in an isolated urban building." Journal of Engineering Mechanics, American Society of Civil Engineers, Reston. ISSN: 0733-9399. 133(8): pp. 887-898.

[14] Yee E., Gailis R. M., Hill A. and Hilderman, T. and Kiel, D. (2006), "Comparison of wind-tunnel and water-channel simulations of plume dispersion through a large array of obstacles with a scaled field experiment." Boundary Layer Meteorology, Springer, Amsterdam. ISSN: 0006-8314. 121(3): pp. 389-432.

[15] Pope S.B. 2000, Turbulent Flows, Cambridge University Press. ISBN: 0521598869.

PROFILES

PROFESSOR ANDY CHAN
He obtained his BEng and PhD from The University of Hong Kong in 1993 and 1997 respectively. His research interest is air pollution dispersion modeling, fluid mechanics and applied mathematics.

MR. ERIC CHEUNG
He obtained his MPhil from The University of Hong Kong in 2006. He is presently a practicing engineer in Hong Kong Productivity Council.

DR PRADEEP G. SIDDHESHWAR
He is Professor of Mathematics at the Bangalore University, India. His current interests are stability of flows, classical instabilities, biomechanics and homotopy methods of solving nonlinear equations. He is equally at ease with analytical and numerical methods.